Supporting Information

Table S1. Joint analysis of Leu+ recombinants.

Table S2. Yeast strains used in this study.

Supplementary Fig. S1. Time course of DSB and repair product formation. (A) Galactose-induced cutting efficiency of the HO cut-sites in the *LEU2* cassette was measured in three strains (XV,V-a, XV,V-b, and V,VIII-2) after pre-growth to exponential phase in YPA glycerol. Cutting efficiencies of the 1st and 2nd cut-sites in the suicide deletion cassette (*i.e.* the two cut sites in the *ade2* allele that flank the *GAL1-HO* gene fusion) were measured in two of the above strains and the values averaged for plotting. Results are expressed as the fraction of intact, *i.e.* unbroken, alleles as compared to a control allele lacking an HO cut-site. **(B)** A yeast strain bearing only the *ade2* suicide deletion cassette was used to measure formation of the suicide deletion NHEJ repair product (right Y axis, open symbols) relative to DSB formation at the 1st cut-site (left Y axis, closed symbols). Yeast were pre-grown either to exponential phase in YPA glycerol (purple), similar to (A), or to saturation in synthetic defined medium for 2 days, similar to the Liquid Galactose plating method (blue).

Supplementary Fig. S2. PCR validation of reciprocal translocations. Leu+ isolates were subjected to PCR using the illustrated primers. PCR products were sequenced to confirm the exact sequence of joints as being primarily precise NHEJ.

Supplementary Fig. S3. *Trans* repair frequencies are not a result of the suicide deletion format. (A) Schematic showing the reporter-based assay to detect reciprocal translocations with ablation of one HO cut site in the *ADE2* suicide deletion cassette. **(B)** *Trans* repair frequency of different strains using the transient galactose method and comparison with galactose plates and liquid galactose methods. Data are the mean ± SD from three or four independent experiments.

Supplementary Fig. S4. Example PCR from competition assay. PCR amplification of Leu+ recombinants using the two indicated sets of primers to discriminate whether the *LEU2* (HYG) or *LEU2* (NAT) cassette was used during competitive *trans* repair.

Supplementary Fig. S5. Deletions of *RAD9* and *RAD51* do not alter observed *trans* NHEJ repair frequencies. Inter- and intra-chromosomal repair assay measuring total survival **(A)** and *trans* repair frequency **(B)** in wild-type, *rad51*Δ and *rad9*Δ strains.

Supplementary Fig. S6. Detailed view of donor locations in HR experiments. (A) Diagram showing the fixed position of the *ADE2* cassette on chrXV and variable positions of the donor sequence in different strains. **(B)** Similar to (A) for the *ADE2* cassette on chrV. **(C)** Similar to (A) for the *ILV1-HOcs* on chrV. Contact frequencies (CF) between the *ADE2* cassette and donor locus are indicated.

Supplementary Fig. S7. Relationship of DSB and donor loci proximity and HR efficiency. Each top panel shows a schematic of the positions of the suicide deletion cassette at the **(A)** *ADE2* locus or **(B)** *CAN1* locus, or **(C)** the *ILV1*-HO cut-site, as well as donor sequences inserted at different places in the genome. Bottom panels show HR efficiency as a function of contact frequency (glycerol-galactose method).

Supplementary Fig. S8. Validation of HR repair by restriction digestion. (A) PCR amplification was performed on DNA from Ade^{-} HR survivors from Fig. S7A using the indicated primers. Products were digested with MluI to confirm that they contain the product expected for HR repair by gene conversion (here the donor contained an MluI site not present in the starting *ADE2* allele). MluI undigested and digested DNAs were run side by side. **(B)** PCR amplification of HR survivors from Fig. S7C using the two indicated primers. Products were digested with PsiI to confirm they contain the product expected for HR repair by gene conversion (here the donor lacked a PsiI site that was present in the starting *ILV1* allele). The first lanes in each row show PsiI digested DNA amplified from the *ILV1* region with the HO cut-site intact. All other lanes show PsiI digested DNA amplified from survivor colonies.

Table S1: Joint analysis of Leu+ recombinants

HO cleavage site (uppercase & underlined) and its flanking sequences, in frame with start codon of ADE2.

agtatggatctcgagGTTTATAAAATTATAC**TGTT**GCGGAAAGCTGAAACTgttgtggaaatgtaa

Strain	Junctional Sequence of Leu2 recombinants	Number of Events
XV,V (ADE2 promoter-Leu2 junction)	GTTTATAAAATTATACTGTTGCGGAAAGCTGAAACT	20
XV,V (HYG-ADE2 coding junction)	GTTTATAAAATTATACTGTTGCGGAAAGCTGAAACT	19
XV,V (HYG-ADE2 coding junction)	No PCR product	1

Table S2: Yeast strains used in this study.

Strains	Genotypes
YW1275	*MATα-inc ade2::HOSD(0)::STE3MET15 his3Δ1 leu2Δ0 met15Δ0 ura3Δ0*
YW2695 (XV,V-a)	YW1275, ChrV, 34kb::*leu2-HYG*
YW2837 (XV,V-b)	YW1275, ChrV, 358kb::*leu2-HYG*
YW2839 (XV,VIII-a)	YW1275, ChrVIII, 314kb::*leu2-HYG*
YW2841 (XV,VIII-b)	YW1275, ChrVIII, 35kb::*leu2-HYG*
YW2843 (XV,XVI)	YW1275, ChrXVI, 126kb::*leu2-HYG*
YW2845 (XV,VI)	YW1275, ChrVI, 39kb::*leu2-HYG*
YW2784 (XV-9kb)	YW1275, ChrXV, 555kb::*leu2-HYG*
YW2788 (XV-110kb)	YW1275, ChrXV, 458kb::*leu2-HYG*
YW2790 (XV-345kb)	YW1275, ChrXV, 223kb::*leu2-HYG*
YW2861	*MATα-inc ade2::URA3 NPR2 prom::ade2::HOSD(0)::STE3MET15 his3Δ1 leu2Δ0 met15Δ0 ura3Δ0*
YW2865 (V,III)	YW2861, ChrIII, 41kb::*leu2-HYG*
YW2867 (V,X)	YW2861, ChrX, 122kb::*leu2-HYG*
YW2869 (V,VI)	YW2861, ChrVI, 39kb::*leu2-HYG*
YW2871 (V,VIII-1)	YW2861, ChrVIII, 314kb::*leu2-HYG*
YW2873 (V,VIII-2)	YW2861, ChrVIII, 35kb::*leu2-HYG*
YW2875 (V,XVI)	YW2861, ChrXVI, 126kb::*leu2-HYG*
YW2903 (V-13kb-R)	YW2861, ChrV, 47kb::*leu2-HYG*
YW2905 (V-153kb)	YW2861, ChrV, 187kb::*leu2-HYG*
YW2907 (V-13kb-L)	YW2861, ChrV, 21kb::*leu2-HYG*

YW2909 (V-358kb)	YW2861, ChrV, 358kb::*leu2-HYG*
YW2877 (XV,V,VI)	YW2837, ChrVI, 39kb::*leu2-NAT*
YW2884 (V,VI,XVI)	YW2869, ChrXVI, 126kb::*leu2-NAT*
YW2893 (V,VI,VIII)	YW2869, ChrVIII, 314kb::*leu2-NAT*
YW2933 (V,VIII,VI)	YW2920, ChrVIII, 314kb::*leu2-HYG*
YW2728	YW2695, *rad9Δ::KanMX4*
YW2732	YW2695, *tel1Δ::KanMX4*
YW2736	YW2695, *dnl4Δ*::*URA3*
YW2953	YW2695, *rad51Δ::KanMX4*
YW2804	YW2790, *rad9Δ::KanMX4*
YW2806	YW2784, *tel1Δ::KanMX4*
YW2808	YW2788, *tel1Δ::KanMX4*
YW2810	YW2790, *tel1Δ::KanMX4*
YW2816	YW2790, *dnl4Δ*::*URA3*
YW2956	YW2790, *rad51Δ::KanMX4*
YW2988	YW2837, *tel1Δ::KanMX4*
YW2990	YW2843, *tel1Δ::KanMX4*
YW2992	YW2869, *tel1Δ::KanMX4*
YW2994	YW2871, *tel1Δ::KanMX4*
YW2996	YW2875, *tel1Δ::KanMX4*
YW2851	YW2695 (*ade2*-cs mut)
YW2853	YW2837 (*ade2*-cs mut)
YW2855	YW2843 (*ade2*-cs mut)
YW726	*MATa ade2::SD0+::URA3 his3Δ1 leu2Δ0 LYS2 MET15 ura3Δ0*
YW2959 (SSA-XV,V-a)	YW726, ChrV, 34kb::*leu2-ISce1-HYG*
YW2961 (SSA-XV,V-b)	YW726, ChrV, 358kb:: *leu2-ISce1-HYG*

YW2963 (SSA-XV,VIII)	YW726, ChrVIII, 314kb:: *leu2-ISce1-HYG*
YW2965 (SSA-XV,XVI)	YW726, ChrXVI, 126kb:: *leu2-ISce1-HYG*
YW3016 (HR-V,XVI)	YW2861, ChrXVI, 126kb::*ade2-HYG*
YW3018 (HR-V,VIII-1)	YW2861, ChrVIII, 314kb::*ade2-HYG*
YW3020 (HR-V,III)	YW2861, ChrIII, 41kb::*ade2-HYG*
YW3022 (HR-V,VI)	YW2861, ChrVI, 39kb::*ade2-HYG*
YW3024 (HR-V,V)	YW2861, ChrV, 358kb::*ade2-HYG*
YW3026 (HR-XV,VI)	YW1275, ChrVI, 39kb::*ade2-HYG*
YW3028 (HR-XV,XVI)	YW1275, ChrXVI, 126kb::*leu2-HYG*
YW3030 (HR-XV,VIII-a)	YW1275, ChrVIII, 314kb::*ade2-HYG*
YW3032 (HR-XV,V-b)	YW1275, ChrV, 358kb::*ade2-HYG*
YW3034 (HR-XV,V-a)	YW1275, ChrV, 34kb::*ade2-HYG*
YW3036 (HR-XV,XV)	YW1275, ChrXV, 223kb::*ade2-HYG*
YW1858	*MATa*-inc::*LEU2 can1*Δ::*ILV1*-QPCR *gal1*::HO *his3*Δ1 *ILV1*prm::HOcs *leu2*Δ*0 met15*Δ*0 ura3*Δ*0*
YW3119 (V,I-1cs)	YW1858, ChrI, 185kb::*ILV1*(2kb) [pGAL1]
YW3121 (V,III-1cs)	YW1858, ChrIII, 41kb::*ILV1*(2kb) [pGAL1]
YW3125 (V,XVI-1cs)	YW1858, ChrXVI, 126kb::*ILV1*(2kb) [pGAL1]
YW3127 (V,VIII-1cs)	YW1858, ChrVIII, 314kb::*ILV1*(2kb) [pGAL1]
YW3129 (V,XIV-1cs)	YW1858, ChrXIV, 293kb::*ILV1*(2kb) [pGAL1]
YW3164 (V,V-1cs)	YW1858, ChrV, 34kb::*ILV1*(2kb) [pGAL1]
YW3166 (V,XII-1cs)	YW1858, ChrXII, 489kb:: :: *ILV1*(2kb) [pGAL1]

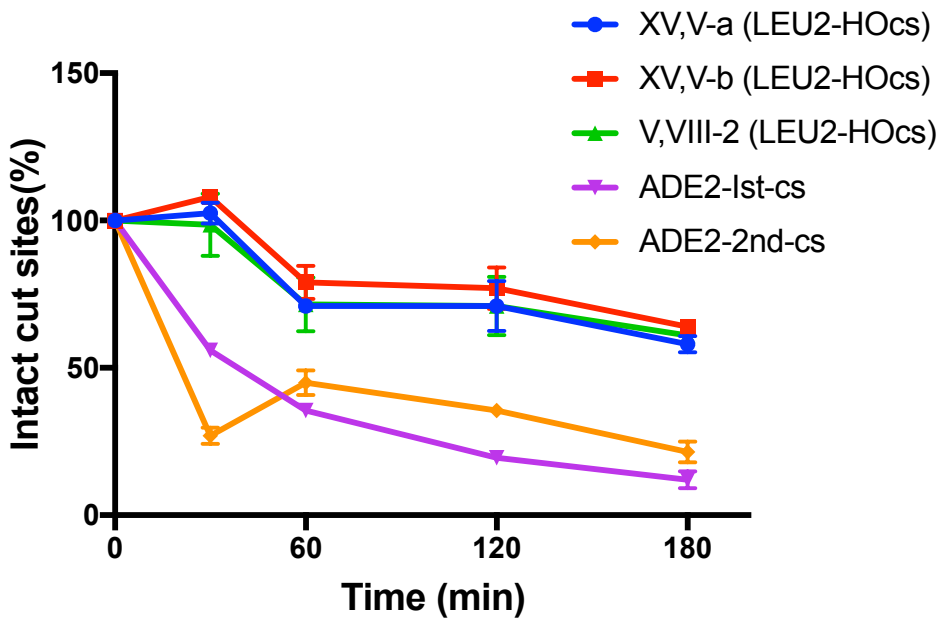

Fig. S1A

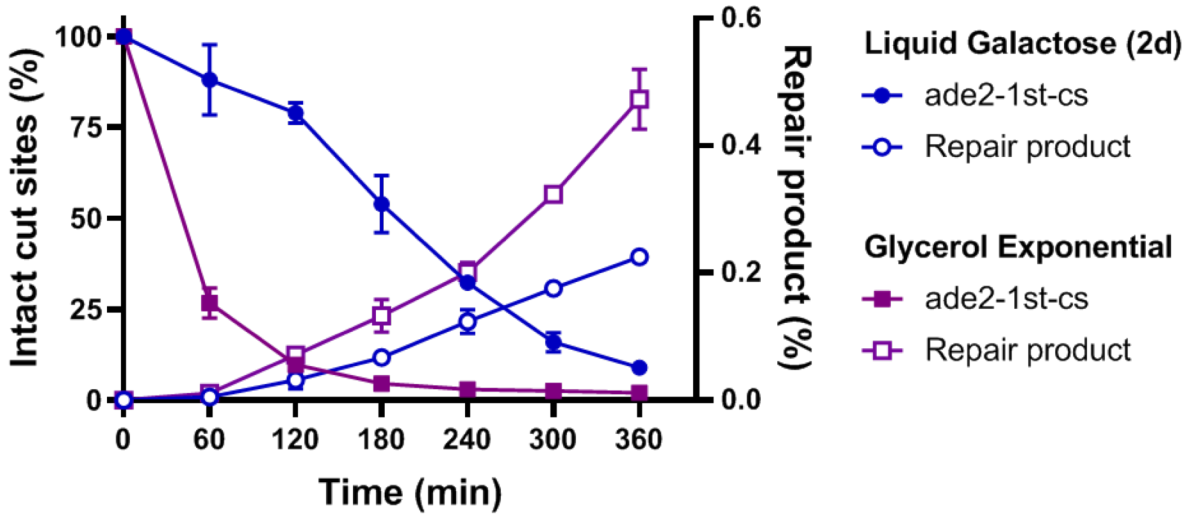

Fig. S1B

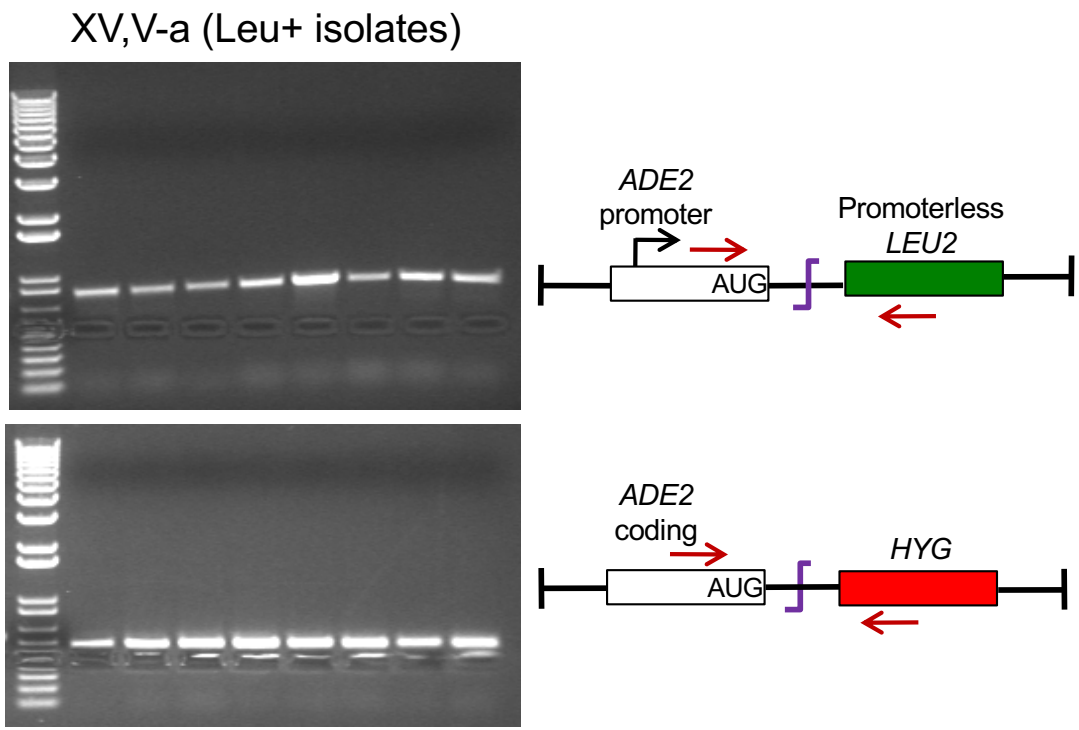
XV,V-a (Leu+ isolates)
ADE2
promoter
Promoterless
LEU2
AUG
ADE2
coding
HYG
AUG

Fig. S2

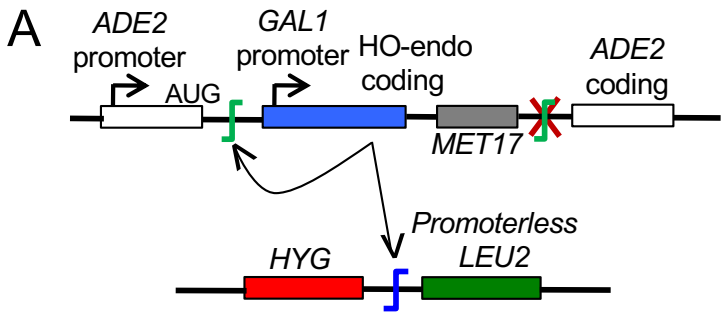
A
ADE2
promoter
AUG
GAL1
promoter
HO-endo
coding
ADE2
coding
MET17
Promoterless
LEU2
HYG

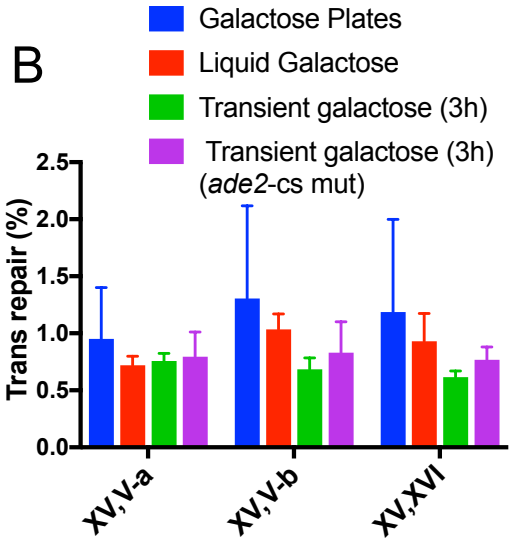
B
Galactose Plates
Liquid Galactose
Transient galactose (3h)
Transient galactose (3h)
(ade2-cs mut)
Trans repair (%)
2.5
2.0
1.5
1.0
0.5
0.0
XV,V-a
XV,V-b
XV,XVI

Fig. S3

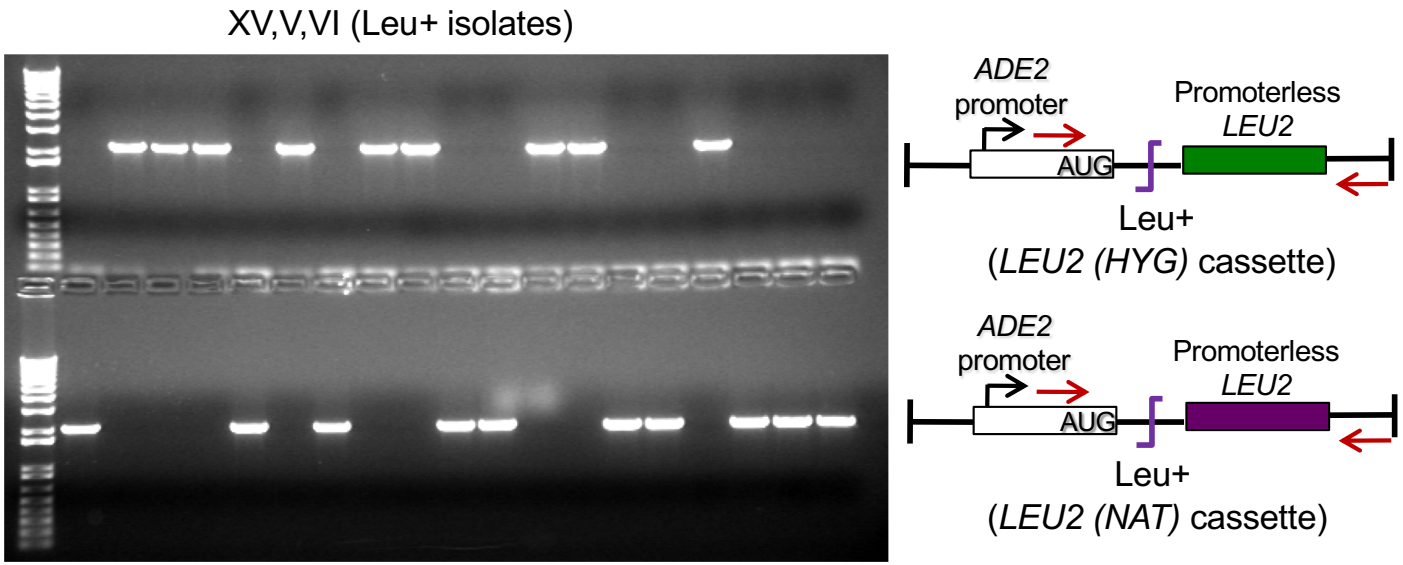
XV,V,VI (Leu+ isolates)
ADE2
promoter
Promoterless
LEU2
AUG
Leu+
(LEU2 (HYG) cassette)
ADE2
promoter
Promoterless
LEU2
AUG
Leu+
(LEU2 (NAT) cassette)

Fig. S4

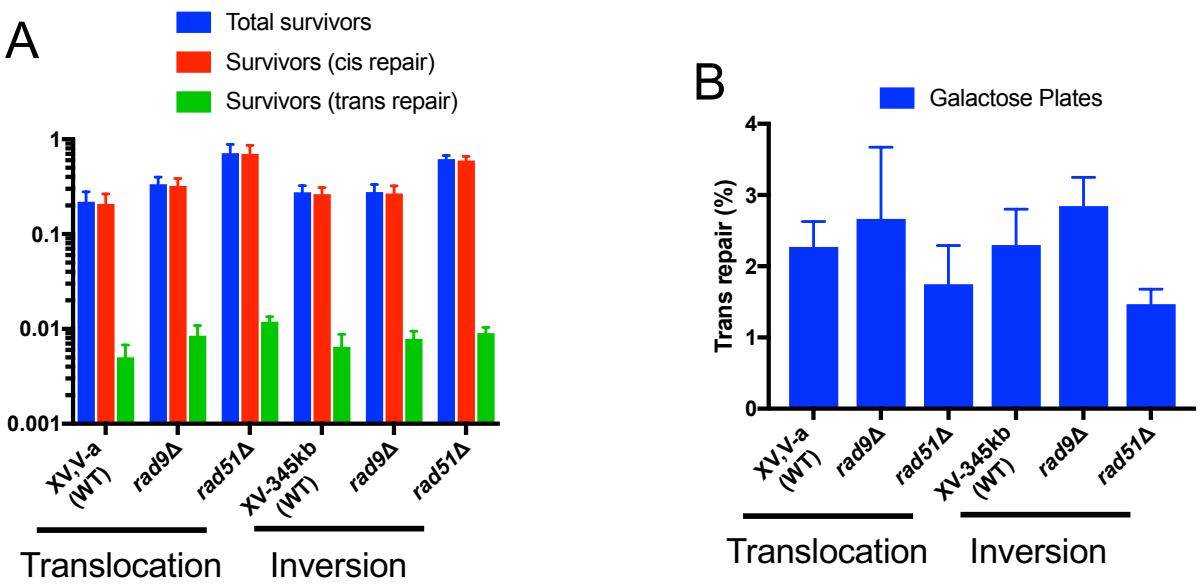
A
Total survivors
Survivors (cis repair)
Survivors (trans repair)
1
0.1
0.01
0.001
XV,V-a (WT)
rad9Δ
rad51Δ
XV-345kb (WT)
rad9Δ
rad51Δ
Translocation
Inversion
B
Galactose Plates
Trans repair (%)
4
3
2
1
0
XV,V-a (WT)
rad9Δ
rad51Δ
XV-345kb (WT)
rad9Δ
rad51Δ
Translocation
Inversion

Fig. S5

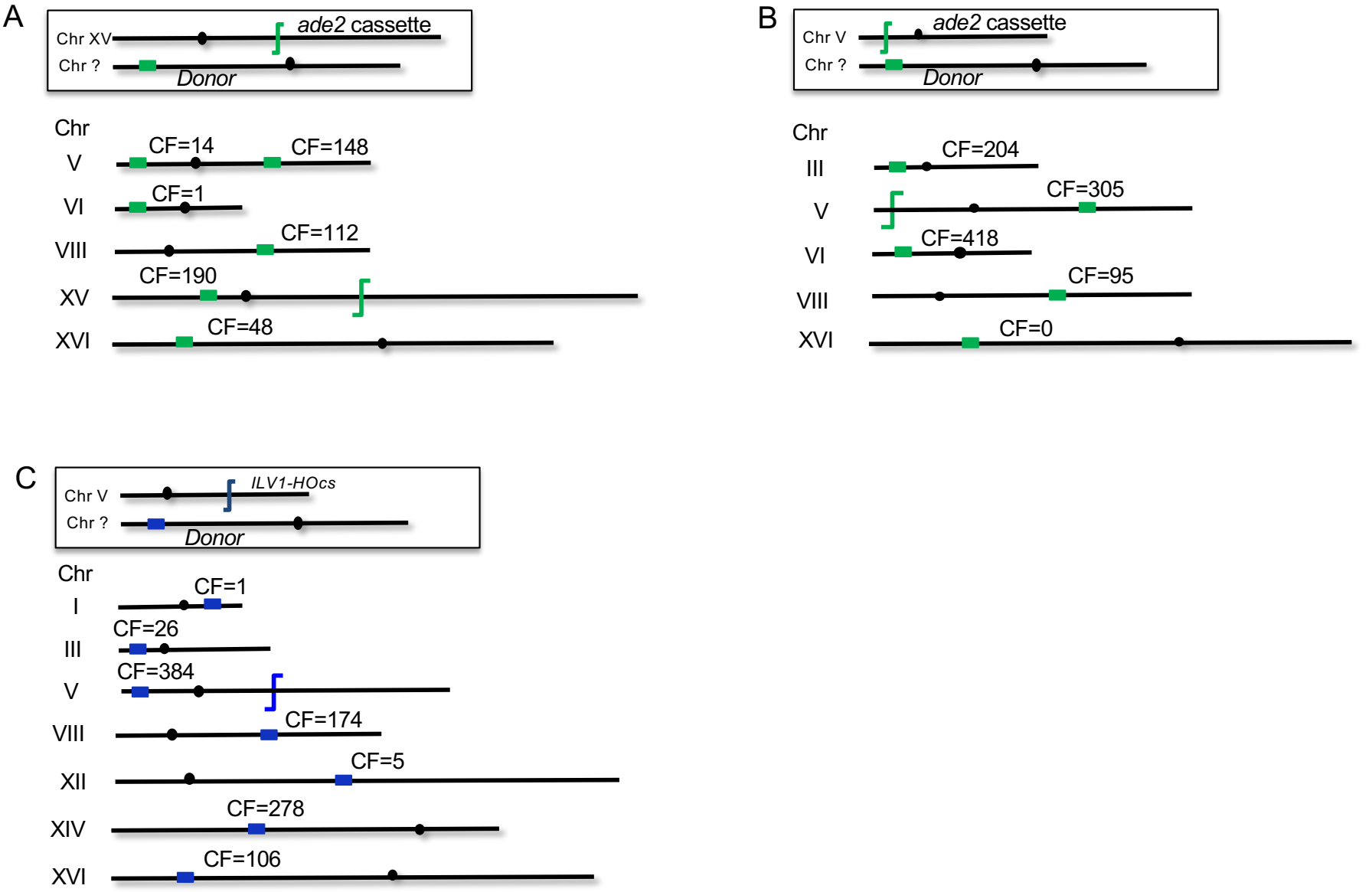
A
Chr XV
ade2 cassette
Chr ?
Donor
Chr
V
CF=14
CF=148
VI
CF=1
VIII
CF=112
XV
CF=190
XVI
CF=48
B
Chr V
ade2 cassette
Chr ?
Donor
Chr
III
CF=204
V
CF=305
VI
CF=418
VIII
CF=95
XVI
CF=0
C
Chr V
ILV1-HOcs
Chr ?
Donor
Chr
I
CF=1
III
CF=26
V
CF=384
VIII
CF=174
XII
CF=5
XIV
CF=278
XVI
CF=106

Fig. S6

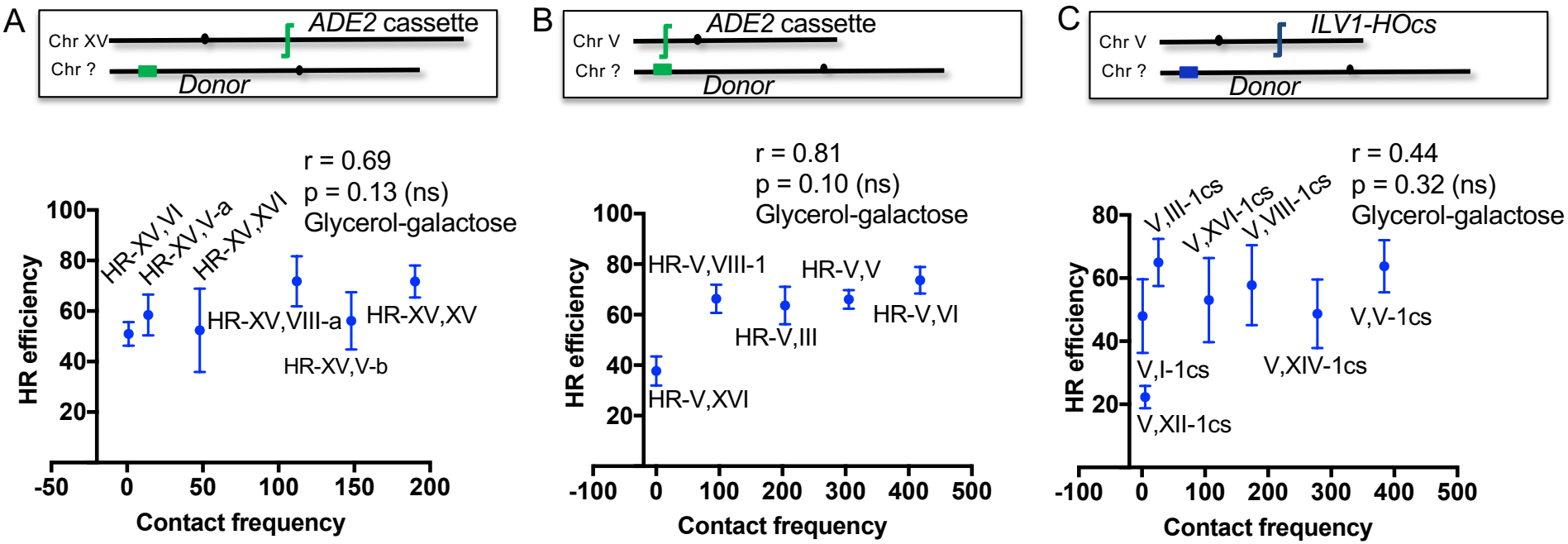
A
Chr XV
Chr ?
ADE2 cassette
Donor
r = 0.69
p = 0.13 (ns)
Glycerol-galactose
HR-XV,VI
HR-XV,V-a
HR-XV,XVI
HR-XV,VIII-a
HR-XV,XV
HR-XV,V-b
HR efficiency
Contact frequency
B
Chr V
Chr ?
ADE2 cassette
Donor
r = 0.81
p = 0.10 (ns)
Glycerol-galactose
HR-V,VIII-1
HR-V,V
HR-V,III
HR-V,VI
HR-V,XVI
HR efficiency
Contact frequency
C
Chr V
Chr ?
ILV1-HOcs
Donor
r = 0.44
p = 0.32 (ns)
Glycerol-galactose
V,III-1cs
V,XVI-1cs
V,VIII-1cs
V,V-1cs
V,I-1cs
V,XIV-1cs
V,XII-1cs
HR efficiency
Contact frequency

Fig. S7

A

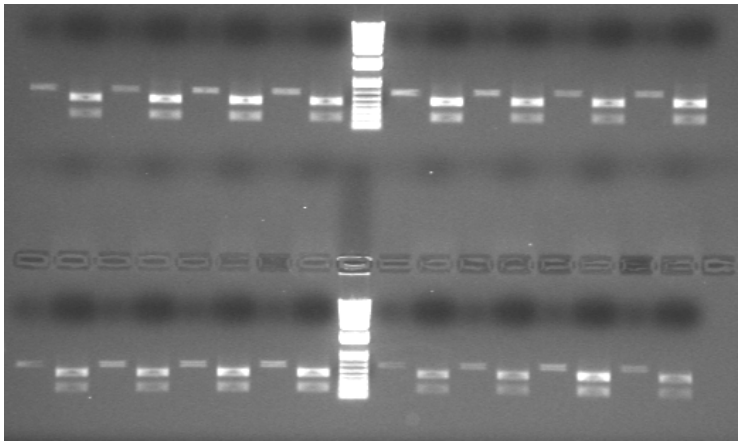

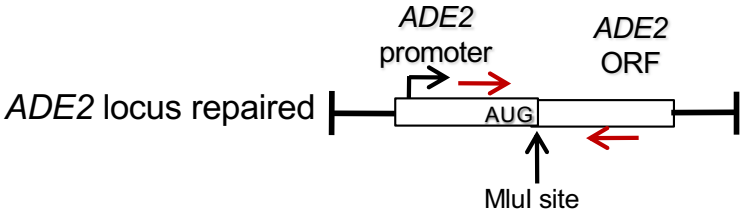
ADE2
promoter
ADE2
ORF
ADE2 locus repaired
AUG
MluI site

B

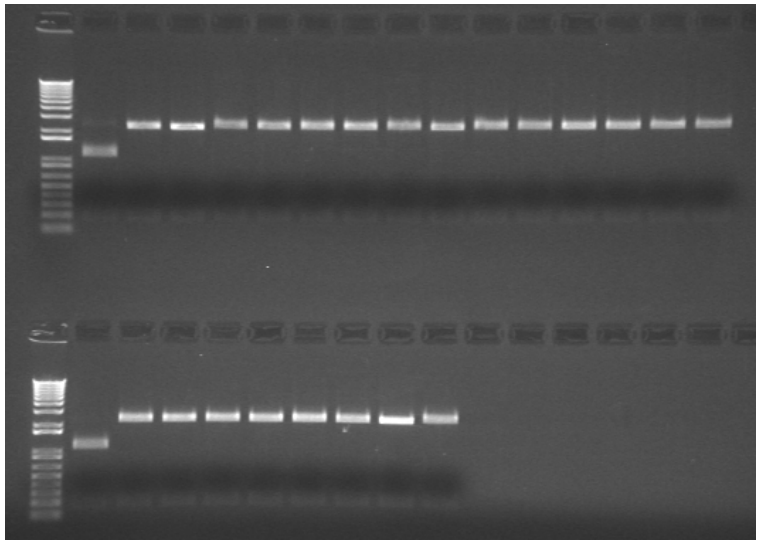

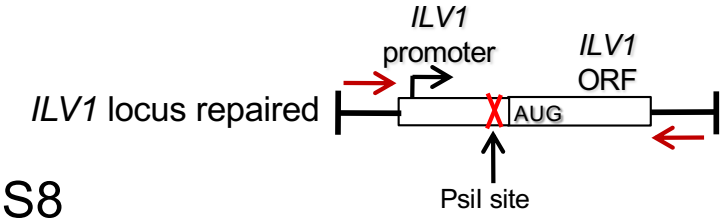
ILV1
promoter
ILV1
ORF
ILV1 locus repaired
AUG
PsiI site

Fig. S8